24

FERMILAB
JAN 8 2001
LIBRARY

GANIL

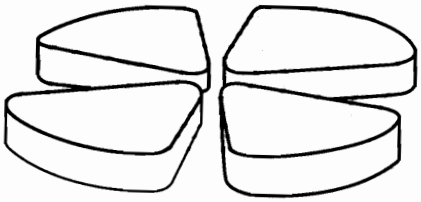

GANIL-P-00-46

Fermilab Library
0 1160 0089369 7

Results and Techniques of Measurements with Inverse Kinematics

W. Mittig and P. Roussel-Chomaz

November 3, 2000

GANIL, BP5027,14076 Caen Cedex 5, France

Submitted to Nuclear Physics
(special issue on Radioactive Nuclear Beams)

GANIL P 00 46

Results and Techniques of Measurements with Inverse Kinematics

W. Mittig and P. Roussel-Chomaz

November 3, 2000

GANIL, BP5027,14076 Caen Cedex 5, France

Abstract

The study of nuclei far from stability interacting with simple target nuclei, such as protons, deuterons, ^{3}He and ^{4}He implies the use of inverse kinematics. The very special kinematics, together with the low intensities of the beams calls for special techniques. Here some examples of the results and techniques used in elastic, inelastic scattering and transfer reactions will be described. Special target techniques and detectors that were developped or are under development in this domain will be described.

1 Introduction

The link between nuclear structure, effective nuclear interactions, nucleon-nucleon potentials and theories such as QCD is still not achieved in a fondamental and quantitative way. In this context, it is very important to get the largest amount of information on nuclear properties in a broad domain. Here we are concerned about nuclei far from stability, where the variable is the isospin, or the difference of neutron and proton numbers (N-Z). The variation of isospin (or more exactly of the z-component of the isospin) has several consequences. When approaching the drip-lines, the binding energy of the last nucleons approaches zero, and this will cause long tails of the wave function at least for low angular momentum. Low density regions of nuclear matter will result, where special correlations may occur. Appropriate measurements, such as elastic scattering, may explore the nuclear interaction in this region.

The spin-orbit interaction is related to surface properties. This is why there are strong presumptions that the spin-orbit interaction and hence magic numbers may change very significantly far from stability. The study of single particle properties by transfer reactions is a privileged tool for this subject.

If we want to study the nature of nuclei far from stability, it is best to have interactions with simple particles, such as electrons, protons and other light particles of well understood structure. The lifetime of the nuclei far from stability being too short to prepare targets in nearly all cases, it will be necessary to inverse the role of target and projectile, and targets of H and He will be needed.

The experiments in this domain need a very good sensitivity in order to detect rare events with high efficiency, combined with high resolution in order to have the maximum of information possible with low statistics. High resolution is often necessary too, to have a very good signal to background ratio in order to find for example a process with one event per day in a background of thousands of events per second.

In the study of reactions in inverse kinematics, the information of interest can be deduced by measuring either the kinematical characteristics of the heavy residue and/or of the light fragment. In the case of the heavy residue, the detection efficiency is increased by the forward focusing of the reaction, and the large velocity allows for the use of relatively thick targets. However, the detection of the heavy fragment is possible only for the reactions where it is bound or has a lifetime long enough to reach the detection system. Moreover, the angular center of mass resolution which can be obtained becomes rather poor, as soon as the mass of the projectile exceeds a few mass units. In these cases, the measurement of the energy and diffusion angle of the light recoil fragment allows to reconstruct the kinematics of the reaction. We will illustrate these considerations by the description of the techniques employed in these experiments and the results obtained.

2 Detection methods

It follows from the angular constraints of the inverse kinematics that a good detection system is the combination of a spectrometer for the forward focussed heavy ion, and of an array of position sensitive silicon detectors for the light particle. We will use the SPEG spectrometer[1] and the MUST array[2], which are currently used at Ganil for the experiments under consideration in the present paper, to give quantitative examples of the experimental achievements and constraints. Similar combinations are used at MSU, whereas RIKEN employs other methods (see below).

2.1 Detection of the heavy residue

In reverse kinematics, the heavy ion is emitted at very forward angles in the laboratory frame. This is an advantage from the point of view of the detection efficiency: a small angular coverage is sufficient to measure a complete angular distribution. For example, with the ± 2 deg angular aperture of SPEG in the horizontal and vertical plane, the angular distribution of elastic scattering for ^{11}Be on proton can be covered with only one angular position of SPEG. However, the kinematic focusing also implies a very good angular resolution in the laboratory angle, in order to achieve even a moderate angular resolution in the center of mass frame. For elastic scattering, detecting the heavy partner,

the rule $\theta_{cm}=\theta_{lab}*(M_{target}+M_{beam})/M_{target}$ is approximately valid. In practice, due to angular straggling in the detectors, the optimum resolution with present detection systems is of the order of one tenth of a degree. With the example of elastic scattering for ^{11}Be on proton, this corresponds to 1.2 deg in the center of mass and to an energy resolution of 200 keV, which is already marginal to clearly separate the first excited state in ^{11}Be at 320 keV. The situation becomes more and more critical as the mass of the projectile increases, which limits the use of spectrometers for the detection of the heavy residue to relatively light projectiles. Another problem arises because of the dispersion in the focal plane of the spectrometer (8 cm/% in the case of SPEG): the kinematics of the reaction varies too rapidly to be covered in a single Bρ setting. The momentum dispersion of a spectrometer allows the measurement of transfer reactions at 0 deg, as illustrated on Figure 1 in the case of the charge exchange reaction p(^{6}He,^{6}Li)n at 41.6 MeV/nucleon. Furthermore, if the spectrometer is operated in energy-loss mode, the energy spread of the secondary beam, usually of the order of 1% or more, is automatically compensated through dispersion matching.

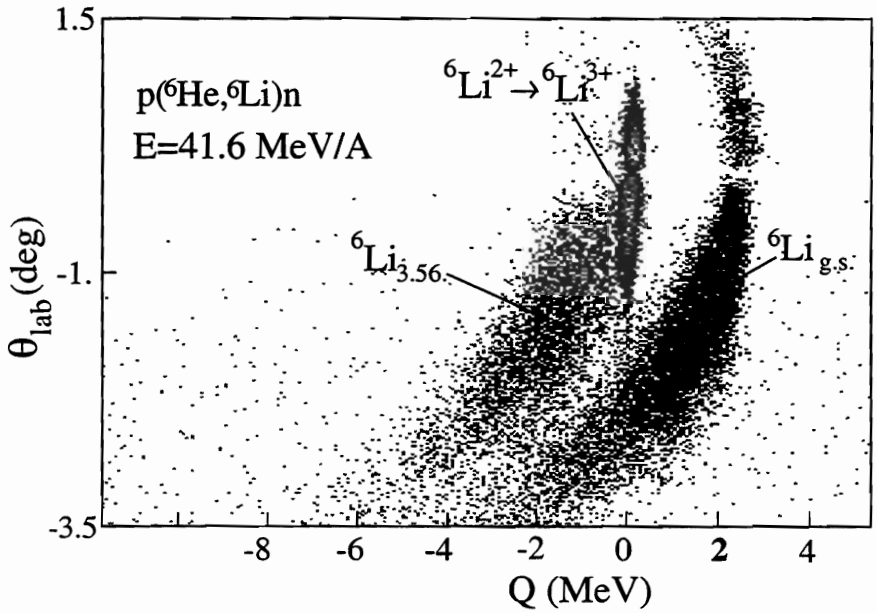

Figure 1: Scatter-plot of the angle versus position in the focal plane of SPEG for the p(^{6}He,^{6}Li)n charge-exchange reaction. The narrow peak corresponds to the stripping in the target of a ^{6}Li^{2+} secondary beam. The other peaks correspond to the (p,n) reaction populating the ground state (right) and IAS (left).

2.2 Detection of the light recoil particle

When the detection of the heavy residue is not satisfying, either because it is not bound or because the angular resolution requirements are too severe, the alternative method is to measure the energy and angle of the recoiling particle. In the case of elastic and inelastic scattering, the light particle is emitted in the forward hemisphere and up to θ_{lab}=90 deg. The measurement of the forward center of mass angles requires a very low energy threshold, of the order of 500 keV for protons. The detectors must therefore cover the energy range from 0.5 up to about 50 MeV protons. The excitation energy resolution depends, too, on the angular resolution in the laboratory frame: to obtain 1 MeV resolution in the case of inelastic scattering of ^{32}Mg on proton, an angular resolution better than 0.5 deg must be achieved. In the case of transfer reactions, the light particles are emitted either at backward (stripping) or forward (pick-up) angles. Here the excitation energy resolution is strongly dependent on the energy resolution of the light particle measurement, which should not be worse than 100 keV. This implies, too, energy losses in the target of the same order or less. The MUST array was designed to meet all these criteria, and to cover a large solid angle. It consists of 8 telescopes composed of a 300μm thick 60x60 mm^2 double sided silicon strip detectors with strips 1mm wide, backed by a 3mm thick Si(Li) detector and a 15mm thick CsI cristal read out by a photodiode. The particle identification is achieved over the full energy range, either by ΔE-E or by ΔE-TOF measurements. The mechanics of the array are modular and can be adapted to various experimental requirements. For example, the experimental set-up used in a recent experiment at GANIL is presented in Figure 2: from right to left, two drift chambers used as beam tracking detectors, the target ladder, and the MUST array divided in two blocks at two symmetric positions around the entrance slits of SPEG.

2.3 Coincidences

In the study of direct reactions, the nuclei of interest are very often lost in a huge background arising for example from break-up processes or from scattered beam particles. This background can be removed by requiring a coincidence with the recoil light particle from the two-body reaction at the appropriate kinematic angle.

A further advantage of the coincidence technique is the separation of events arising from the transfer reaction on hydrogen from those arising from the same reaction on other constituents of the target, for example carbon in the case of a polymer target.

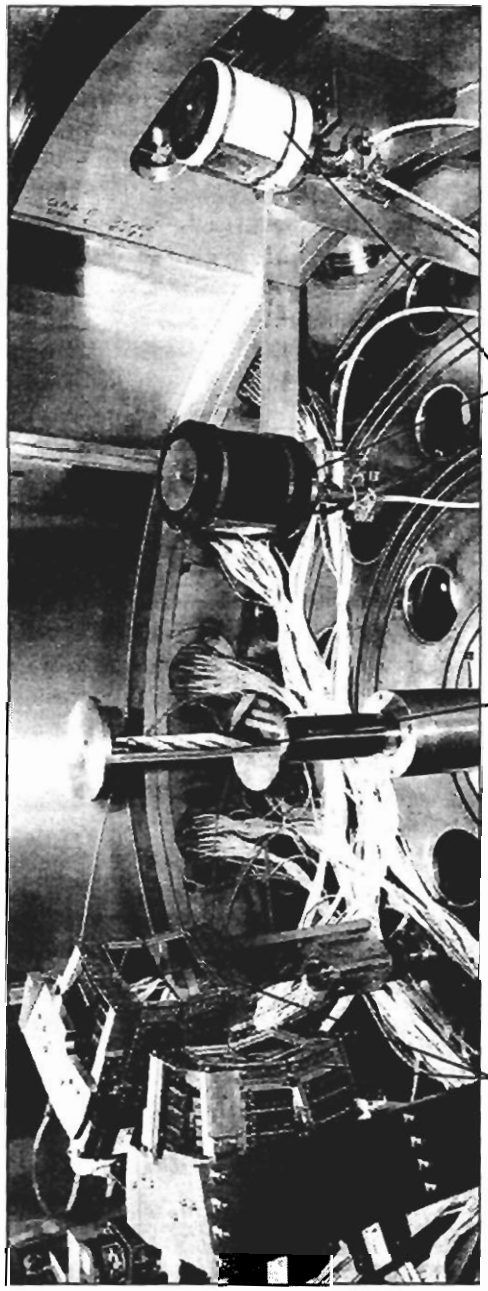

Figure 2: Experimental set up in the SPEG reaction chamber.

2.4 Beam tracking detectors

The experiments performed with secondary beams produced by fragmentation are faced to two main difficulties: the low intensity of the beams, which can be partly compensated by using detection set-ups with high angular coverage, and their poor optical qualities. This problem is solved by the measurement of the angular and/or energy characteristics of each incident particle, which is made possible by the low intensity of the secondary beams. Beam tracking detectors have been developed, which are able to stand counting rates up to 10^6 pps, and which allow to reconstruct the incident angles with a resolution similar to that of the reaction products detectors. For example at Ganil, these beam tracking detectors are of three types. With drift chambers filled with isobutane at 20 mbar, the position is measured by the drift time of the electrons. The measurement of the angle is obtained with two detectors distant by roughly 1 m. Each detector consists of 4 individual drift chamber modules, two for the horizontal position (right and left), and two for vertical position (up and down). Their active area is 70x70 mm^2. With the use of multi-hits electronics, the efficiency of such detectors is 75 to 80% for a counting rate up to $8x10^5$ pps[3].

The second type of beam tracking detectors consists of two low pressure multiwire proportional chambers with one plane of anode wires placed between two cathode planes, respectively segmented into 28 vertical or horizontal strips, 2.54 mm wide. The anode wires deliver a time signal allowing a time of flight measurement with an accuracy between 500 ps and 1.2 ns, depending on the energy loss of incident particle in the detector. The cathode strips are individually read out and the position of incoming particles is reconstructed using a charge centroid finding algorithm[4]. For both type of detectors the spatial resolution is better than 1 mm, even at high counting rate.

For particles with $Z \geq 8$, μchannel devices have very good efficiency and very thin detector foils (≤ 100 $\mu g/cm^2$). They are at the moment the detector system which causes the minimum perturbation of the particle characteristics. Detectors of the other types have typically thicknesses of at least 1 mg/cm^2. Spatial resolution achieved is better than 1 mm, if magnetic focusing of secondary electrons is used[5].

3 Target Techniques

3.1 Cryogenic targets

The need of simple targets implies the use of H, D,^{3,4}He. H and D can be used as chemical compounds, and polyethylene, CH_2 and CD_2, is commonly used. Due to the carbon in this compound, for the same energy loss, the target contains 3 times less hydrogen than would be possible for a pure hydrogen target.

The Carbon provokes a background that either must be determined by making a measurement with a pure C target, or must be eliminated by coincidences. For He the only possibility is a gas or liquid target.

In these cases an entrance window is necessary. The thickness of this undesired window will be proportional to the pressure. Thus in order to increase the target thickness for a given window, the only way is to decrease the temperature. Standard coldheads for cryogenic pumps go down to about 15K. This implies a gain of a factor 20 with respect to room temperature. For H and D, it is most convenient to work somewhat above the critical point for the coexistence of liquid-gas, at about 30K. For a 1cm thick target at 30K and 5atm, 5mg/cm^2 of H_2 are obtained. At this pressure a 10μm Havar window is needed for a diameter of 20mm.

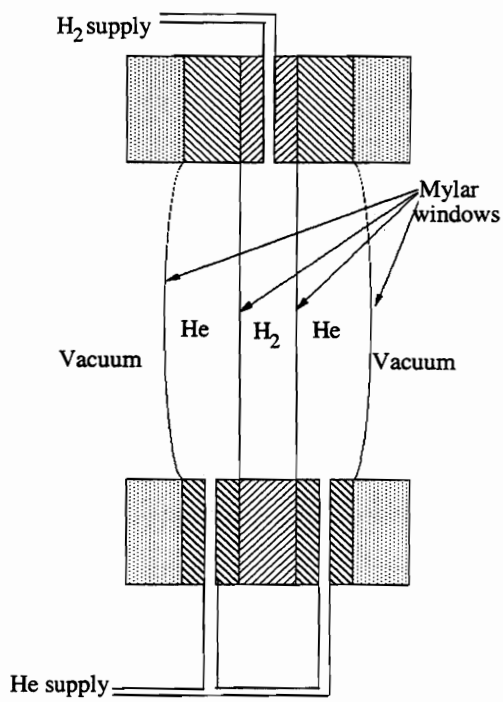

Figure 3: Schematic vue of the target that allows formation of homogeneous solid H_2 or D_2 without window deformation.

For thicker targets, either liquid or solid targets should be used. The filling of the target implies high pressures, in the case of H_2 at least 100mb are necessary to remain above the triple point(coexistence of vapour, liquid and solid at 14K

and 70mbar). To avoid window deformations that will result in inhomogeneous targets, two methods have been used. The first one is to use a mold, that confines the H_2 during solidification in a well defined volume. This method was tested at Riken[6]. At Ganil we tested another method using a double window illustrated on Figure 3 [7]. During the formation of the solid hydrogen, a pressure of He of exactly the same value as in the inner cell maintains the inner windows free from constraints. Once the solid is formed, the He can be taken out. The total window thickness can be as low as about 1mg/cm^2 of mylar. Hydrogen thicknesses down to 1mm corresponding to 7mg/cm^2 can be achieved.

The phase transition in this target observed during cooling down is shown on Figure 4.

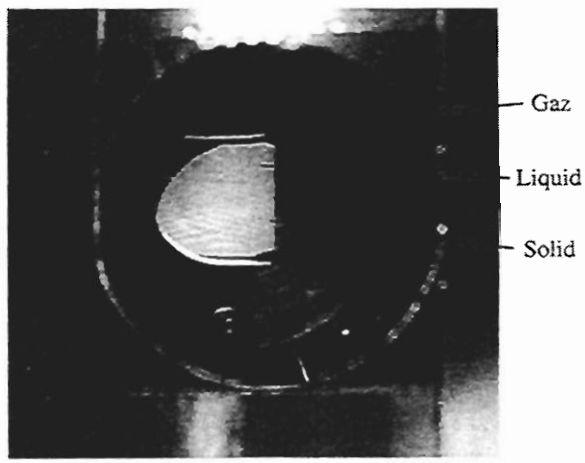

Figure 4: Phase transition in the cryogenic target schematized on Figure 3 [7].

3.2 Active targets

The problem of loss of resolution due to thick targets can be avoided by the use of active targets, this is, the target is simultaneaously a good resolution detector. Effectively, H_2, D_2, and He are good detector gases. By the detection of the scattered particle and the recoiling target nucleus a 100% efficient 4π detection is achieved. The archetype of such a detector is IKAR[8], that was recently used to measure high quality data of elastic scattering of e.g. ^{4,6,8}He at 700MeV/nucleon[9].

Once again, low temperature may be used to achieve high target density. The price to pay for such high densities is the very long drifttime of the electrons in

the gas if reasonable fields are applied.

As an example we show on Figure 5 an energy spectrum obtained with a small ionisation chamber at 10atm of hydrogen at 30K[10].

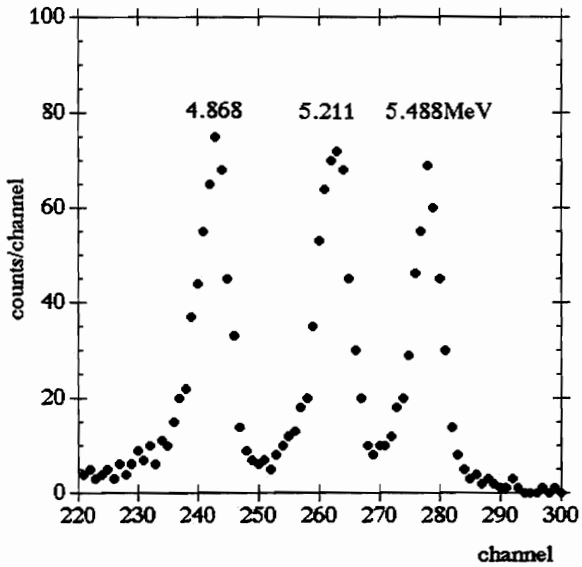

Figure 5: Pulse height spectrum obtained with a 3 peak α source in a high pressure(10atm), low temperature(30K) ionisation chamber. The resolution is 80keV(FWHM).

4 Elastic, inelastic scattering and charge exchange reaction

Elastic scattering with stable nuclei provided most of the available information on the nuclear interaction potential, especially in the case of light projectiles, where both phenomenological[11, 12, 13, 14] and microscopic [15, 16] optical potential models have been developed to describe experimental results[17, 18, 19]. With the secondary beams, these studies have gained renewed interest, since it became possible to measure elastic scattering for nuclei lying far from stability, and to compare the potentials developed for stable nuclei with the ones obtained for these exotic nuclei. These elastic scattering experiments constituted a first generation of experiments, with rather large cross sections, possible with the low intensity of the secondary beams. They are, too, a first step, necessary and important to obtain the interaction potentials needed to

analyse inelastic scattering or transfer reaction cross sections.

In particular many experiments were devoted to the study of halo nuclei[9, 20, 21, 22, 23, 24], for which the weak binding energy is expected to lead to modifications of the optical potential. The first results showed that the angular distributions obtained for light neutron rich nuclei such as ^{9}Li, ^{10}Be could be very well reproduced with the global parametrisation CH89[11], or within the JLM approach[15] by using HF or gaussian density distributions with the usual normalisation factors for real (λ_v=1.0) and imaginary (λ_w=0.8) potentials [21](see Figure 6). However the cross sections for neutron halo or skin nuclei such as ^{6}He, ^{8}He, ^{11}Li or ^{11}Be were systematically overestimated by the calculated angular distributions. To obtain a good description of the data, the interaction potential had to be modified either by reducing the real part or increasing the imaginary part. This effect was interpreted as a manifestation of break up processes which should be important for these loosely bound nuclei.

New data on ^{6}He elastic scattering[25] measured more recently over a greater angular range, with the MUST array were analysed in conjunction with the charge exchange reaction p(^{6}He,^{6}Li$_{IAS}$)n angular distribution[26] and the reaction cross-section for the system ^{6}He+p[27] at energy close to 40 MeV/nucleon. These results show that, by using density distributions which include the halo effect[28, 29], all these experimental results can be very well reproduced within the JLM approach, with only a slight normalisation of the real and imaginary potentials (λ_v=0.9, λ_w=0.85) , but an important increase of the isovector part of the interaction (λ_{iv}=1.4), thus confirming the previous conclusions concerning the underestimation of the isovector part in the JLM approach[30]. The inelastic scattering data to the first 2^+ excited state, measured by detecting the recoil protons in the MUST array show a remarkable sensitivity to the halo structure of ^{6}He over the entire angular distribution[25], contrary to elastic or charge exchange reaction which are sensitive to the detailed structure of the wave function only at very large angles.

In the case of ^{6}He, the elastic scattering on a ^{4}He gas target measured at 25 MeV/nucleon at JINR Dubna[23] showed a backward rise in the cross sections, which could be reproduced by taking into account a two-neutron exchange mechanism. The DWBA calculations presented on Figure 7 use the ^{6}He ground state wave function estimated within a three body model (α+n+n)[31] which presents two distinct spatial components: a di-neutron and a "cigar-like" component. These calculations show that the 2-neutron exchange can be very well accounted for with the di-neutron configuration, and that the cigar-like component contributes only negligibly to the backward rise. Such an effect was not observed in the elastic scattering of ^{8}He on ^{4}He[32].

Elastic scattering at high energy has also been measured to obtain quan-

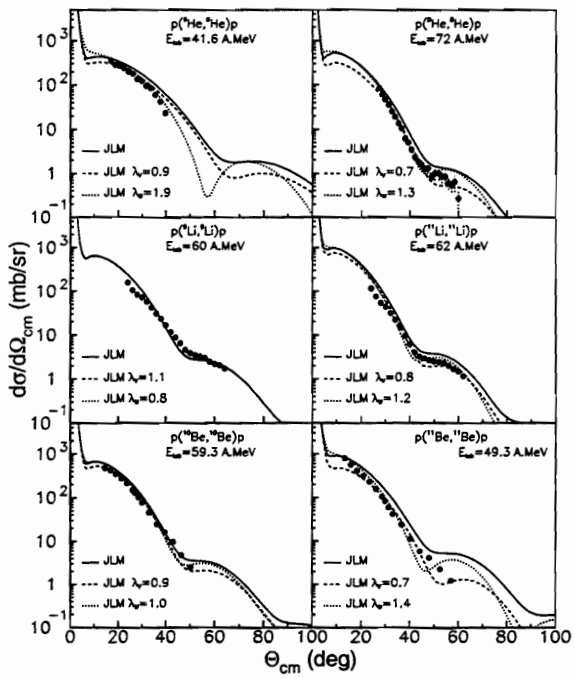

Figure 6: Measured elastic scattering angular distributions compared to calculations performed within the JLM approach. The data are from [20, 21, 22]. The solid curves correspond to the standard JLM normalisation, the dashed (dotted) lines to the best fit obtained when the real (imaginary) part of the potential is adjusted.

titative information on the radial shape of exotic nuclei. Indeed, the Glauber scattering theory allows to connect the investigated nuclear distributions to the measured cross section in a quite direct way[33].

Elastic scattering of He isotopes has been measured at 700 MeV/nucleon on protons inside the hydrogen filled ionisation chamber IKAR which served simultaneously as gas target and recoil detector[9]. From the slope of the differential cross section $d\sigma/dt$, the matter radii of ^{4,6,8}He have been deduced, which are in close agreement with the values obtained from reaction cross sections[34]. Since the difference between the elementary pp and pn cross sections is small at this energy, the sensitivity of the calculated p-nucleus cross section to the difference between the proton and neutron density distributions is also rather weak. The values deduced from such experiments on the neutron distributions rely therefore on some assumptions for the proton distributions, for example that the protons are contained only in the core of the halo nucleus. However,

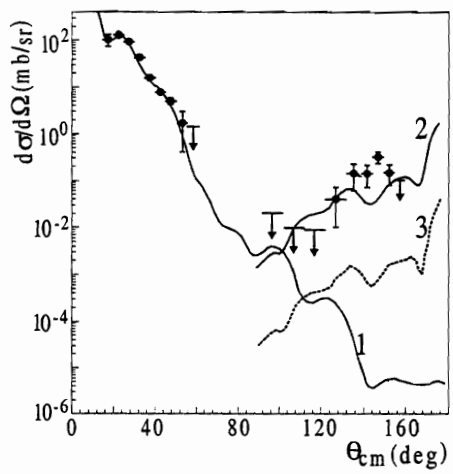

Figure 7: Elastic scattering angular distribution measured for ^{6}He+^{4}He at 25 MeV/nucleon(from ref. [23]). Curve 1 corresponds to the angular distribution calculated with WS parameters very close to those obtained for the system ^{4}He+^{6}Li. Curve 2 shows the cross section calculated for the transfer with the full wave function, and curve 3, with the di-neutron component removed.

concerning the matter radii extracted from the data, the authors of Ref.[9] claim that the fact that they are the same for the four density distributions considered, shows that this determination is model independent. This affirmation is contested by studies which show that reaction calculations are highly sensitive to the details of the wave function inputs beyond their r.m.s. radii[35]. By considering few-body approach which includes cluster correlations and realistic 2n-halo asymptotics[36], the r.m.s. matter radius deduced for ^{6}He was 2.5 fm instead of 2.3 fm found in the minimally correlated density distribution used in [9]. This result confirms the increased transparency observed in reaction cross section calculations which include an explicit treatment of the few-body nature of halo nuclei [37].

Some experiments were devoted to the study of inelastic scattering in reverse kinematics on light targets[22, 25, 38]. This kind of measurement is complementary to those obtained by Coulomb excitation because electromagnetic excitation mainly probes the protons in the nucleus, while in proton, or more generally low-Z targets, inelastic scattering, it is the nuclear excitation which is dominant. By combining the two types of measurements, it is possible to

separate the neutron and proton deformation. These studies are useful, too, to establish the level scheme of nuclei at the limits of stability. Most of the very light neutron rich nuclei have only a bound ground state. Therefore inelastic scattering studies proceed via two experimental methods: the recoil particle detection or the invariant mass reconstruction where the decay products of the excited unstable nucleus are detected in coincidence.

Both methods were used to search for excited states in ^{8}He[22]. An exited state at $E^* = 3.57 \pm 0.12$ MeV, $\Gamma = 0.5 \pm 0.35$ MeV was observed, in good agreement with previous results using multiple transfer reactions with stable beams[39]. From the analysis of the angular distribution $J^\pi = 2^+$ was assigned to this state. Another possible structure was seen at $E^* \sim$ 5-6 MeV, but with very low statistics.

Inelastic scattering of ^{11}Li + p was also studied [38] by detecting in coincidence the recoil protons, charged particles and the neutrons resulting from the breakup of ^{11}Li. The coincidence spectra show a clear peak at $E^* = 1.3 \pm 0.1$ MeV, $\Gamma = 0.75 \pm 0.6$ MeV. The angular distribution measured for this state corresponds to L=1. On the basis of orbital momentum composition of ^{9}Li and the two neutrons of the halo, this state is found consistent with quantum number in the system n+n+^{9}Li $J^\pi = 0^-$ or 1^- (omitting the intrinsic spin of ^{9}Li). The conclusion was that the ground state of ^{11}Li cannot have a structure with valence neutrons in pure s orbital, but must contain some component of the $p_{1/2}$ orbital.

Elastic and inelastic scattering was also studied for heavier nuclei such as the oxygen, sulfur and argon isotopes on protons[40, 41, 42, 43, 44]. In this case, the detection of the scattered beam would require an angular resolution in the laboratory system which was not achievable and therefore both elastic and inelastic scattering angular distributions were measured by the detection of the recoiling protons in coincidence with the projectile or its residue. The results obtained for inelastic scattering to the first 2^+ state in ^{20}O are particularly interesting[43]. By combining the proton scattering data with electromagnetic measurements, an experimental value of the neutron to proton multipole matrix elements M_n/M_p could be deduced. The experimental value of this ratio for the 2^+ states changes very rapidly from ^{18}O where $M_n/M_p \sim N/Z$ as expected for a purely isoscalar transition, to ^{20}O where this ratio is much larger than N/Z. This observation demonstrates the isovector character of the 2^+ excitation, driven by the neutrons, and the rapid change in the nature of the excitation, as a function of increasing number of the valence neutrons.

5 Transfer Reactions

Transfer reactions have been since several decades an essential tool for single particle nuclear structure studies. They allow to determine the level schemes of nuclei, even if they are located beyond the drip line. The transferred momenta,

and subsequently the spins and parities of the states can be deduced from the shape of the angular distributions, while the spectroscopic factors and therefore the probability of finding a nucleon in a given shell model orbit. Hence, one-nucleon transfer reactions are especially well suited to study shell effects in nuclei, since the exchange of one nucleon between the projectile and target populates selectively one-particule or one-hole nuclear states. Secondary beams with reasonable intensities made a new generation of experiments achievable, where transfer reactions on light targets are used to study the spectroscopy of nuclei at the limit of stability and even beyond. The cross sections for single tranfer are sufficiently large to perform these experiments with secondary beams of intensity as low as a few 10^4 pps. DWBA and coupled channel calculations have demonstrated in the past the reliability of their predictions for transfer reactions, so that the experimental results can be interpreted unambiguously.

The first experiments performed up to now have been interested mainly in (p,d), (d,^{3}He),(p,2p) reactions, i.e. neutron or proton pick-up, or stripping reactions such as (d,p). The nuclei of interest are the light most neutron rich nuclei such as ^{5,7}H, ^{7,9}He, ^{11}Be.... We will review the results obtained up to now on these very exotic nuclei, by order of increasing atomic number.

5.1 Hydrogen isotopes

The question of the possible existence of superheavy hydrogen isotopes is debated since many years, with conflicting results: various attempts to observe either a stable or resonant state of ^{5}H yielded negative results[45], while the observation of ^{5}H among the products of reactions with pions[46, 47] and with stable (^{6}Li)[48] and radioactive (^{6}He)[49] was claimed, but with values of the energy and the width varying from one experiment to another. For ^{7}H, no experimental evidence of a resonant state has been reported so far. Very recently, (p,2p) reaction was used to produce ^{5}H (resp. ^{7}H) with ^{6}He (resp. ^{8}He) beams at Dubna (resp. RIKEN) bombarding the GANIL gas target[50], 10mm thick, filled with pure hydrogen at a pressure of 11 atm and temperature of 35K[51]. The target windows were 10 μm stainless steel foils. Figure 8 presents a schematic drawing of this cryogenic target. The RIKEN telescope involving 8 annular Si-strip detectors detected the proton pairs from the (p,2p) in an angular range between 10 and 18 deg. The experiment performed at RIKEN is presently under analysis. As for the Dubna experiment, the energy of the ^{5}H nucleus was deduced from the energies and angles of the two correlated protons detected in coincidence with the triton resulting from the decay $^5\mathrm{H} \rightarrow \mathrm{n+n+}^3\mathrm{H}$ at the most forward angles. This is analog to the missing mass method where the recoil particle (here the virtual state ^{2}H) is unstable. Figure 9 presents the energy distribution obtained for the ^{5}H system when the coincidence with ^{3}H was required (left) or not (right). The resonant state of ^{5}H is clearly seen as a maximum at $\sim$ 2 MeV above the threshold for $^5\mathrm{H} \rightarrow \mathrm{n+n+}^3\mathrm{H}$ decay. The bump

on the right side of the spectra is due to phase space volume which produces a distribution of events limited on the left by zero energy and on the right by the energy threshold of the detectors. The thin line for the spectrum without the ^{3}H coincidence shows the background obtained with the hydrogen gas evacuated from the target. Only few background events were obtained when the coincidence was required.

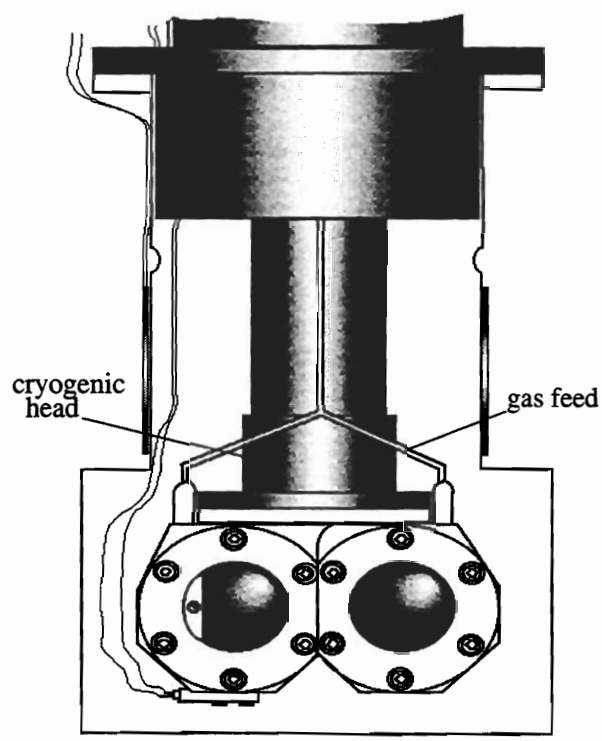

Figure 8: Cryogenic target. The two parts of the target have different thicknesses: 1cm (left) and 0.5 cm (right). From ref. [50].

5.2 Helium isotopes

Among the odd neutron rich He isotopes, which are all unbound, ^{7}He was studied repeatedly since many years. Its ground state resonance is well known, but no excited state could be observed until recently. It is expected that the first excited state has a neutron $1p_{1/2}$ configuration. The first possible observation of an excited state in ^{7}He with E*=3.16 MeV, Γ=1.5 MeV was reported in

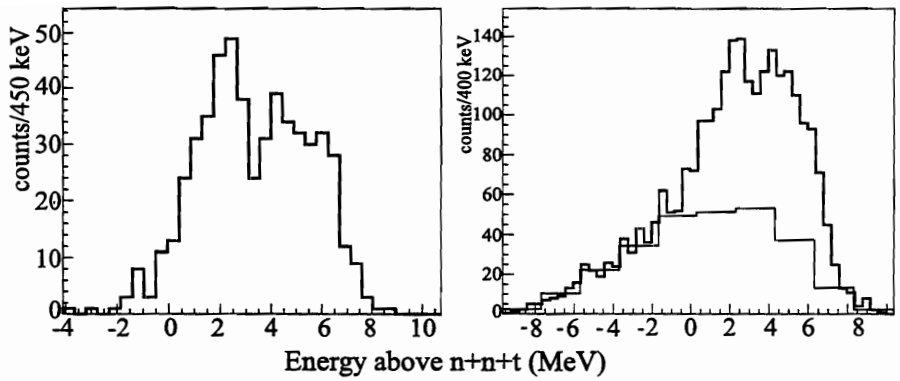

Figure 9: Energy distribution obtained for the ^{5}H system formed in the reaction ^{6}He(p,2p) when the coincidence between the two protons and ^{3}H resulting form the decay of ^{5}H was required (left) or not (right). From ref. [51].

transfer reactions with stable beams ^{9}Be(^{15}N,^{17}F)^{7}He [39]. Almost simultaneously an excited state was observed in ^{7}He via the (p,d) reaction induced by ^{8}He secondary beam at RIKEN on a CH_2 target[52]. The experimental set-up used in this experiment is displayed on Figure 10. Multiwire proportional chambers were used as beam tracking detectors. The RIKEN telescope, placed at forward angles, detected the deuterons. The charged particles resulting from the decay of ^{7}He were bent in the dipole magnet and identified by the drift chamber and the plastic scintillators of the hodoscope, while the neutrons were detected in a neutron wall of plastic scintillators. With the coincidence between the deuteron and the decay products of ^{7}He, an excited state was observed at E*=2.9 $\pm$ 0.3 MeV with Γ= 2.2 $\pm$ 0.3 MeV. Its characteristics are in relatively good agreement with the results of [39]. It decays mainly into 3n+^{4}He, in spite of the larger n+^{6}He decay energy. This observation is consistent with a structure for this state of a ^{6}He core in 2^+ state coupled to a $1p_{1/2}$ neutron. The population of such a state with unusual structure via ^{8}He(p,d) reaction confirms that the ground state wave function of ^{8}He is dominated by the configuration with a ^{6}He subsystem in the 2^+ exited state [52].

The pick up reaction d(^{6}He,^{7}He)p was also used to search for new excited states in the ^{7}He nucleus[51]. In this reaction, a relatively high population probability, comparable to that of the ground state, for the single particle $1/2^-$ state is expected via a single step transfer. The experiment was performed on ACCULINNA at JINR Dubna with the Ganil gas target operated with deuterium at 3 atm and 40K. Three annular Si-Strip detectors from the RIKEN telescope were installed at backward angles (θ_{lab}=154.3-170.7 deg) to detect low energy protons (E=2.5-6 MeV) emitted at small center of mass angles in (d,p) reaction.

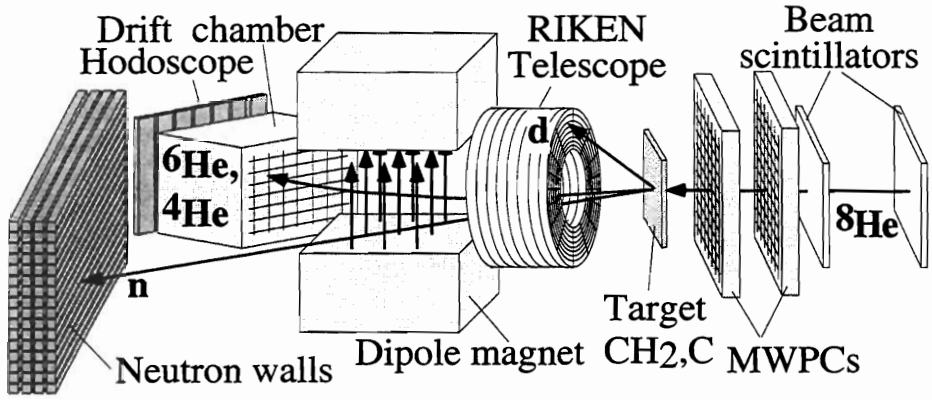

Figure 10: Experimental setup used at RIKEN. From ref. [52].

The peak corresponding to the ^{7}He ground state resonance was very clearly seen in this experiment, and the underlying background was negligible. However, no other resonance could be observed in the excitation energy region extending up to 8 MeV, which indicates that ^{7}He does not have well pronounced narrow excited states with single particle structure.

5.3 The structure of ^{11}Be ground state

One characteristic feature of the ^{11}Be nucleus is the parity inversion observed for its ground state which has $J^\pi = 1/2^+$ in contradiction to simple shell model and spherical Hartree Fock predictions of $1/2^-$. The recent calculations[53, 54, 55, 56, 57, 58, 59] of the ^{11}Be ground state structure correctly reproduce this parity inversion, and describe the ground state in terms of coupling between the ^{10}Be core states and the valence neutron. However their predictions concerning the degree of coupling of an $s_{1/2}$ neutron to the ^{10}Be ground state relative to the coupling of a $d_{5/2}$ neutron to a ^{10}Be core in its first 2^+ state vary by one order of magnitude. A direct test of the models can be provided by the measurement of the relative cross sections feeding the 0^+ and 2^+ states of ^{10}Be. For this purpose the p(^{11}Be,^{10}Be)d reaction was studied with the high resolution magnetic spectrometer SPEG at GANIL[60, 61]. The energy and scattering angle of ^{10}Be fragments were measured in the focal plane of SPEG in coincidence with deuterons detected with the CHARISSA array[62] located in the reaction chamber between 5 and 35 deg. Figure 11 presents the ^{10}Be spectra in singles (top) and in coincidence with the deuterons (bottom). The black spectrum superimposed on the upper panel is a spectrum taken on carbon target, normalised to the same number of beam particles and equivalent target thickness.

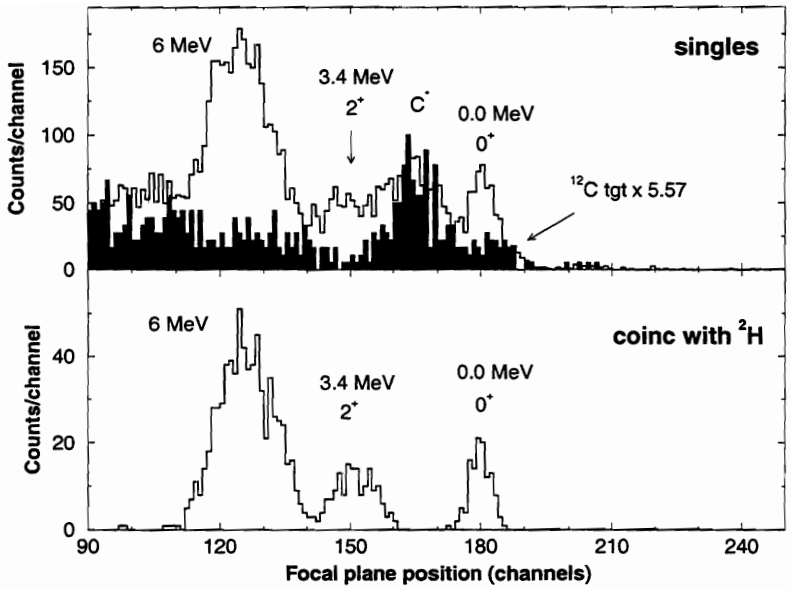

Figure 11: ^{10}Be focal plane spectra, in singles (top), and in coincidence with deuterons (bottom).From ref. [61].

A first DWBA analysis with single particle form factor gave a core excitation admixture larger or equal to 30%. However more refined calculation of the form factors within the particle vibration coupling model[56, 57] show that the radial wave function of the $d_{5/2}$ transferred neutron is strongly modified by the ^{10}Be deformed core. The coupled channel calculations performed with these form factors enhance significantly the cross sections for the $2^+ \otimes 1d_{5/2}$ configuration compared to the single particle form factors. The present "best estimate" of the ^{11}Be ground state wave function is a dominant $[0^+ \otimes 2s_{1/2}]$ component with a 0.16 $[2^+ \otimes 1d_{5/2}]$ core excitation admixture. This result is in good agreement with other recent ones obtained from high energy knock-out reactions with a ^{11}Be beam[63], from the measurement of magnetic moment of ^{11}Be at ISOLDE[64] and finally from new reaction calculations which deduce from the reaction cross section values the average radius of the halo and subsequently the percentage of s-wave component in the ^{11}Be wave function[65]. All these results confirm that the s-wave function is dominant in ^{11}Be ground state with a d-wave admixture of at most 20%.

6 Association of direct reactions and γ detection

It is trivial to say that in a direct reaction it is necessary to determine which is the final state populated, however this is difficult to realise experimentally. A resolution in the final state energy of the order of 100keV is needed. If the heavy reaction product is detected, this implies a high $\Delta E/E$ resolution, e.g. 10^{-4} in the case of A=20 at 50MeV/nucleon. This is difficult to achieve with the large emittance of secondary beams and the thick targets needed. This difficulty can be overcome when γ rays are detected. As an example we show the results of a knock-out reaction studied at MSU [63]. The beam was ^{11}Be, hitting a ^{9}Be target, that was surrounded by a 4π NaI γ detector. The ejectile after abrasion of one neutron, ^{10}Be, was observed at zero degrees with a magnetic spectrograph, the S800. The Doppler corrected γ spectrum is shown on Figure 12. From this spectrum the cross-sections for the different levels, including the ground state, were deduced, taking into account the possible cascades. The cross sections obtained were, within the errors, compatible with spectroscopic factors predicted by a shell model calculation, of 0.74 and 0.18 for the configurations $[0^{+}\otimes 2s_{1/2}]$ and $[2^{+}\otimes 1d_{5/2}]$ respectively. This result is in good agreement with the one obtained in the (p,d) reaction discussed before.

7 Conclusion and Perspectives

Experimental sensitivity was greatly increased during the last decade thus allowing detailed direct reaction cross section studies down to intensities of 10^2 to 10^4 radioactive ions per second.The fact that the nucleus under study is the projectile calls for simple target nuclei, such as p,d,^{3}H,^{4}He, and most efficiently these targets can be provided by cryogenic techniques, already used or under development. Many results have already been obtained, mainly for light nuclei, enlightning many of the special features of nuclei near drip lines. These light nuclei have strong cluster structures that could be studied. For mean field properties far from stability, it will be more suited to study heavier nuclei with A$\geq$20. Together with upgrades of beam intensities, higher resolution and even higher efficiency will be needed. Cheaper high granularity detectors and electronics will help to develop such devices. Active targets will be needed to be able to work with thick targets without loosing resolution. Spectrometers at 0 deg will be used for tagging and background reduction. The resolution necessary to resolve discrete nuclear states in inverse kinematics by the detection of the heavy residue is difficult to achieve due to the need of thick targets. This difficulty may be overcome by the use of active targets. Coincidence with γ devices is and will be an important tool to resolve states. High granularity is necessary to reduce strong Doppler broadening in inverse kinematics. Knock-out reactions at intermediate energy complement lower energy pick-up reactions in inverse kinematics.

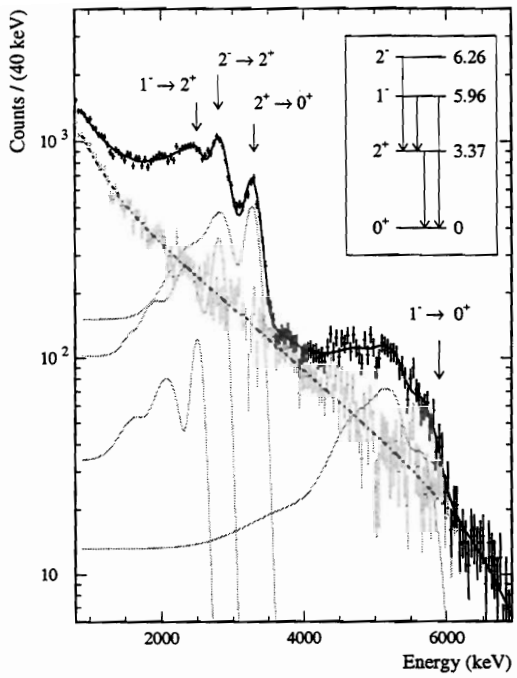

Figure 12: Doppler corrected energy spectrum measured with the NaI array in coincidence with ^{10}Be fragments of a 60MeV/nucleon ^{11}Be beam, detected in the magnetic spectrometer. The solid curve is the final fit to the data, and contains the sum of the simulated response functions (gray curves) for the four γ energies indicated (see insert too), and a background parametrisation (dashed dotted line).From ref. [63].

The combination of elastic, inelastic scattering and transfer reactions will enable us to explore the properties of weak radioactive beams, pushing our knowledge to the edge of the nuclear chart.

References

[1] L. Bianchi et al., Nucl. Inst. Meth. A 276 (1989) 509

[2] Y. Blumenfeld et al., Nucl. Inst. Meth. A 421 (1999) 471

[3] M. Mac Cormick et al., Ganil report R 98 02 (1999)

[4] S. Ottini-Hustache et al., Nucl. Inst. Meth. A 431 (1999) 476

[5] O.H. Odland et al., Nucl. Inst. Meth. A 378 (1996) 149

[6] S. Ishimoto et al., KEK Preprint 2000-23H

[7] P. Dolegeviez, private communication

[8] J.P. Burq et al., Nucl. Phys. B 217 (1983) 285

[9] G.D. Alkhazov et al., Phys. Rev. Lett. 78 (1997) 2313

[10] H. Savajols, private communication

[11] R.L. Varner et al., Phys. Rep. 201 (1991) 57

[12] F.D. Becchetti and G.W. Greenlees, Phys. Rev. 182 (1969) 1190

[13] E.D. Cooper et al., Phys. Rev. C 47 (1993) 297

[14] S. Hama et al., Phys. Rev. C 41 (1990) 2737

[15] J.P. Jeukenne, A. Lejeune and C. Mahaux, Phys. Rev. C 16 (1977) 80

[16] F.A. Brieva and J.R. Rook, Nucl. Phys. A 307 (1978) 493

[17] J.S. Petler et al., Phys. Rev. C 32 (1985) 673

[18] S. Mellema et al., Phys. Rev. C 28 (1983) 2267

[19] L.F. Hansen et al., Phys. Rev. C 31 (1985) 111

[20] C.B. Moon et al., Phys. Lett. B 297 (1992) 39

[21] M-D. Cortina-Gil et al., Phys. Lett. B 401 (1997) 9

[22] A.A. Korsheninnikov et al., Phys. Lett. B 316 (1993) 38

[23] G.M. Ter-Akopian et al., Phys. Lett. B 426 (1998) 251

[24] V. Lapoux et al., Proc. Soloviev99, Int. Symposium on quasiparticle and phonon excitations in nuclei, RIKEN, Japan (1999)159

[25] F. Auger et al., Proc. ENPE 99, Seville, Spain (2000)

[26] M-D. Cortina-Gil et al., Nucl. Phys. A 641 (1998) 263

[27] A. de Vismes et al., submitted for publication

[28] S. Karataglidis et al., Phys. Rev. C 61 (2000) 024319

[29] K.Arai et al., Phys. Rev. C 59 (1999) 1432

[30] F.S. Dietrich and F. Petrovich, in proceedings of Neutron-Nucleus Collisions-a probe of nuclear structure, eds J. Rapaport et al., AIP Conference Proceedings, no124 (AIP, New York 1985) p 90

[31] M. Zhukov et al., Phys. Rep. 231 (1993) 151

[32] R. Wolski et al., Proc. Int. Conf. on Radioactive Nuclear Beams RNB5, April 3-8 2000 Divonne, Switzerland (World Scientific, Singapore, 2000)

[33] R.J. Glauber, Lectures in Theoretical Physics, Interscience, New York, 1959, Vol. I

[34] I. Tanihata et al., Phys. Lett. B 289 (1992) 261

[35] J.A. Tostevin and J.S. Al-Khalili, AIP Conference Proceedings 455. ENAM 98 (1998) 227

[36] J.S. Al-Khalili and J.A. Tostevin, Phys. Rev. C 57 (1998) 1846

[37] J.S. Al-Khalili and J.A. Tostevin, Phys. Rev. Lett 76 (1996) 3903

[38] A.A. Korsheninnikov et al., Phys. Rev. Lett 78 (1997) 2317

[39] H.G. Bohlen et al., Prog. in Part. Nucl. Physics 42 (1999) 17

[40] F. Marechal et al., Phys. Rev. C 60 (1999) 034615

[41] F. Marechal et al., Phys. Rev. C 60 (1999) 064623

[42] J.K. Jewell et al., Phys. Lett. B 454 (1999) 181

[43] E. Khan et al., Phys. Lett. B 490 (2000) 45

[44] E. Khan et al., submitted for publication

[45] A.A. Oglobin and Yu.E. Penionzhkevich, Treatise on Heavy Ion Science, Ed. D.A. Bromley, Volume 8 Nuclei far from stability, Plenum Press, New York and London, 1989, p.261

[46] K.K. Seth, Proc. Int. Conf. On Nuclei far from Stability, Helsingor, Denmark, 1981, CERN 81-90, 1981, p.655

[47] M.G. Gornov et al., Nucl. Phys. A 531 (1991) 613

[48] D.V. Aleksandrov et al., Proc. Int. Conf. on Exotic Nuclei and Atomic Masses, Arles, France, 1995, Eds. M. de Saint-Simon and O. Sorlin. Editions Frontieres, Gif sur Yvette Cedex France, 1995, p. 329

[49] T. Kobayashi et al., Nucl. Phys. A 616 (1997) 223c

[50] J-F. Libin and P. Gangnant, Ganil report Aires 01-97 (1997)

[51] M.S. Golovkov et al., Proceedings of the Conference "Nuclear Structure and Related Topics", Dubna, June 6-10, 2000

[52] A.A. Korsheninnikov et al., Phys. Rev. Lett. 82 (1999) 3581

[53] E.K. Warburton and B.A. Brown, Phys. Rev. C 46 (1992) 923

[54] T. Otsuka, N. Fukunishi and H. Sagawa, Phys. Rev. Lett 70 (1993) 1385

[55] P. Descouvemont, Nucl. Phys. A 615 (1997) 261

[56] N. Vinh Mau, Nucl. Phys. A 592 (1995)33; N. Vinh Mau and J.C. Pacheco Nucl. Phys. A 607 (1996) 163

[57] T. Bhattacharya and K. Krishan, Phys. Rev. C 56 (1997) 212

[58] F.M. Nunes, I.J. Thompson and R.C. Johnson, Nucl. Phys. A 596 (1996) 171

[59] H. Esbensen, B.A. Brown and H. Sagawa, Phys. Rev. C 31 (1993) 1274

[60] S. Fortier et al., Phys. Lett. B 461 (1999) 22

[61] J. Winfield et al., to be published in Nucl. Phys.

[62] R.L. Cowin et al., Nucl. Inst. Meth. A 423 (1999) 75

[63] T. Aumann et al., Phys. Rev. Lett 84 (2000) 35

[64] W. Geithner et al., Phys. Rev. Lett. 83 (1999) 3792

[65] J.A. Tostevin, Proc. 2nd Int. Conf. on Fission and neutron rich nuclei, St Andrews, Scotland, ed. J. Hamilton, W.R. Phillips and H.K. Carter (World Scientific, Singapore, 2000) p 429